Computational Intelligent Gait-Phase Detection System to Identify Pathological Gait

Chathuri M. Senanayake and S. M. N. Arosha Senanayake, *Senior Member, IEEE*

***Abstract*—An intelligent gait-phase detection algorithm based on kinematic and kinetic parameters is presented in this paper. The gait parameters do not vary distinctly for each gait phase; therefore, it is complex to differentiate gait phases with respect to a threshold value. To overcome this intricacy, the concept of fuzzy logic was applied to detect gait phases with respect to fuzzy membership values. A real-time data-acquisition system was developed consisting of four force-sensitive resistors and two inertial sensors to obtain foot-pressure patterns and knee flexion/extension angle, respectively. The detected gait phases could be further analyzed to identify abnormality occurrences, and hence, is applicable to determine accurate timing for feedback. The large amount of data required for quality gait analysis necessitates the utilization of information technology to store, manage, and extract required information. Therefore, a software application was developed for real-time acquisition of sensor data, data processing, database management, and a user-friendly graphical-user interface as a tool to simplify the task of clinicians. The experiments carried out to validate the proposed system are presented along with the results analysis for normal and pathological walking patterns.**

***Index Terms*—Fuzzy inference system (FIS), gait-phase detection, hardware and software codesign, virtual instrumentation.**

I. Introduction

GAIT analysis is the study and investigation of human locomotion, which is carried out by visual observation, sensor technology, video/optical cameras, or integration of these methods.

With the development of microtechnology, microsensors such as accelerometers, gyroscopes, magnetometers, load cells, foot switches, electromyography (EMG) sensors, etc., are readily available in the industry that can be utilized for human-gait analysis. It is a crucial factor to identify sensor types to obtain reliable and accurate data based on the application. Therefore, many research works have been carried out to investigate the feasibility of these sensor types in physical rehabilitation [1]–[5].

Initial research studies on gait analysis revealed that a walking gait cycle can be divided into eight phases, namely initial contact (IC), loading response (LR), mid-stance (MSt), terminal stance (TSt), preswing (PSw), initial swing (ISw), mid-swing (MSw), and terminal swing (TSw) [6]–[8]. Gait-phase detection is mostly used to determine accurate timing of corrective feedback in rehabilitation.

Gait phases of a healthy human are continuous and always follow the aforementioned sequence. In the presence of abnormalities, the gait phases will present irregularities. Therefore, differentiating gait phases is also known as an effective method to detect gait anomalies.

Many simple algorithms are presented by researchers to distinguish between gait phases [9]–[11]. Smith *et al.* [11] proposed a threshold-based gait-phase detection system that differentiated gait phases based on foot-pressure patterns. The results reported that 80% of the detection errors were due to failure of the force-sensitive-resistor (FSR) signal not reaching the threshold value. In recent years, more sophisticated computer technology is integrated into the field of biomechanics to design feasible gait-phase detection algorithms incorporating artificial intelligence such as neural network, fuzzy logic, and hybrid systems [12]–[15]. The detection errors reported in [12] was addressed in [16] and [17], where Kong *et al.* used fuzzy logic to determine gait phases of walking based on foot-pressure patterns. The authors report that the use of fuzzy logic helps obtain full information on gait patterns even at the presence of low sensor signals.

Although many algorithms are present, the accuracy and reliability of these algorithms still remain questionable, and a standard accepted gait-phase detection algorithm is not yet present. Therefore, this paper investigates the reliability and accuracy of an intelligent gait-phase detection system using both foot-pressure and joint-angle measurements incorporated with machine intelligence (fuzzy logic). The gait-phase detection algorithm was developed using the concept proposed by Kong and Tomizuka [16]. However, this system only used foot-pressure information that was sufficient only to detect subphases of the stance phase. Therefore, in this paper, in addition to FSRs, two inertial sensors are proposed in order to detect subdivisions of both swing and stance phase.

The main objective of the proposed system is to obtain accurate measurements for efficient detection of gait phases during walking gait. In contrast to existing systems, this paper presents an overall hardware and software codesign of a wearable smart device for gait-phase detection with the competence to be used in a clinical environment.

II. Design and Implementation of the System

A. Hardware and Software Codesign

The overall system can be presented as an integration of software and hardware implementation (see Fig. 1). The hardware consists of four FSRs, two inertial measurement units (IMUs),

Manuscript received June 9, 2009; revised March 17, 2010; accepted July 2, 2010. Date of current version September 3, 2010. This work was supported by Monash University, Sunway campus, and by the Ministry of Science, Technology, and Innovation (MOSTI) Malaysia, under Grant 03–02-10-SF0028 with the title "Bio-Inspired Robotics Devices for Sportsman Screening Services (BIRDSSS)."

The authors are with the School of Engineering, Monash University, Sunway Campus, Jalan Lagoon Selatan, Bandar Sunway, 46150 Petaling Jaya, Selangor, Malaysia (e-mail: chathuri4@gmail.com; aroshas@ieee.org).

Digital Object Identifier 10.1109/TITB.2010.2058813

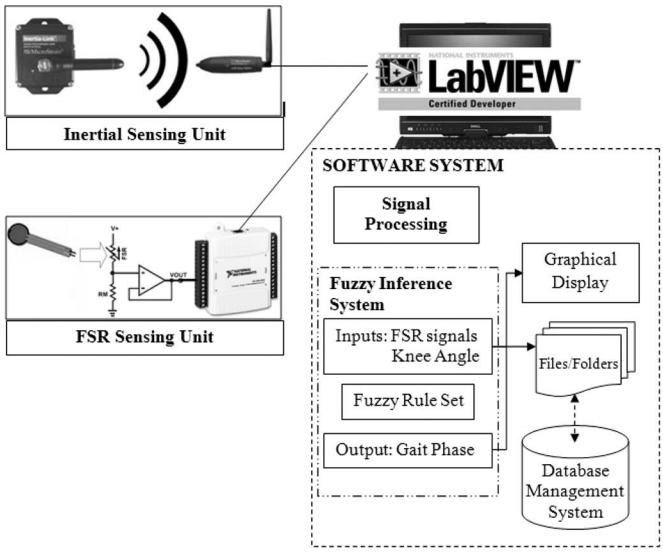

Fig. 1. Overall system architecture.

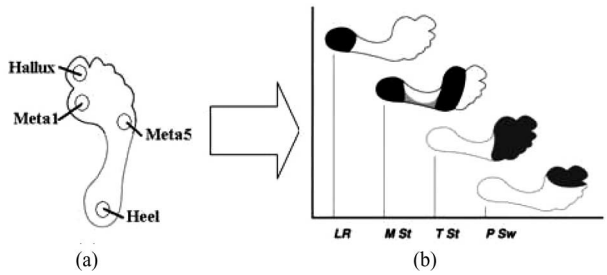

Fig. 2. (a) FSR sensor placements at the heel, Meta5, Meta1, and hallux. (b) Foot-pressure patterns with shaded areas representing pressure occurrences for each subphase of stance phase.

and data-acquisition (DAQ) devices to obtain foot-pressure patterns and Euler angles of the knee joint during walking. Four FSRs from Interlink Electronics were placed in a shoe insole of size 8 (average shoe size of test subjects) to avoid damage to sensors and ensure comfort of the wearers. FSRs are polymer-film devices, which exhibit a decrease in resistance with an increase in the force applied to the active surface [18]. The FSRs used consist of circular sensing area with 0.5 in diameter and a negligible thickness of 0.018 in.

Inertia Link offered by Microstrain, Inc., is an IMU that combines a triaxial accelerometer, triaxial gyro, temperature sensors, and an on-board processor. This wireless sensor comes with a 2.4-GHz universal-serial-bus (USB) base station that allows efficient data transfer from the sensor to host PC. This sensor was utilized for the sole purpose of obtaining accurate measurements of the knee-joint angle of the human walking gait.

The FSR signals were transmitted to the host PC by means of a USB DAQ device (NI-USB-6009) by National Instruments (NI). The four FSR sensor signals were tied to the analog inputs of the DAQ device for continuous DAQ. Furthermore, a conditional circuit was built to convert the applied force to readable voltage values. The overall wearable system is portable due to its small size and light weight. The system can be used with minimal setup time due to its plug-and-play capabilities.

The primary software used was LabVIEW by NI. The built-in libraries of LabVIEW were used to acquire sensor data via the DAQ devices, and to perform signal processing and filtering to obtain foot-pressure patterns and knee angle. These two gait parameters were used as inputs to the fuzzy inference system (FIS) to detect gait phases of walking in real time. A user-friendly graphical-user interface (GUI) was also implemented in LabVIEW for users to interact with the hardware setup, and graphically represent the gait parameters and gait phases detected. The sensor data are also saved in files for later reference and are linked to a database that manages the patients personal and trial records. The FIS was initially designed using the fuzzy logic toolbox available by MATLAB. The developed FIS was imported to LabVIEW to enable real-time capabilities.

In contrast to most systems, the software application itself performs signal processing/filtering that reduces the overall hardware to be tied to the wearer.

B. Differentiation of Gait Phases Based on Gait Parameters

The foot-pressure patterns and the knee angle for each gait phase during walking were obtained with reference to normative data presented in [6]–[8]. The maximum pressure occurs at the heel, first metatarsal head (Meta1), fifth metatarsal head (Meta5), and the hallux, which are identified as the joints with maximum force occurrence during walking [16]. With reference to Fig. 2(b), the darkened area represents the joints where pressure occurs for each subphase of the stance phase. Therefore, it was concluded that four FSRs placed at the aforementioned joints were sufficient to detect subphases of stance phase, namely LR, MSt, TSt and PSw.

The FSRs placed at heel, Meta5, Meta1, and hallux will be referred to as FSR1, FSR2, FSR3, and FSR4, respectively, for the rest of the content of this paper [see Fig. 2(a)].

Fig. 3(b) illustrates the knee angle during normal-walking gait [6]. The knee passes through four arcs during one gait, and knee flexes and extends in alternately. The third and the fourth arcs represent the knee-angle pattern during the swing phase. The latter two arcs are considered in this paper to differentiate gait phases during the swing phase, namely the ISw, MSw, and TSw of a gait cycle. The range of knee angle for each phase can be used to differentiate between phases which are represented within vertical lines shown in Fig. 3(b). The knee angle was chosen to develop the FIS as the knee mobility and stability are major factors in the normal-walking pattern and it is the junction of the femur and tibia that constitute to the major segments of the lower limb [6].

To obtain accurate measurements of the knee angle during walking gait, two IMUs were placed at the thigh and the shank with the *Y*-axis pointing into the page. The sensors A and B in Fig. 3(a) should be placed such that it gives a negative and positive value, respectively, when rotated clockwise. The Euler angles obtained from these two sensors were summed to obtain the knee angle represented in Fig. 3(b) "θ," which is the angle of rotation of the shank with respect to the thigh.

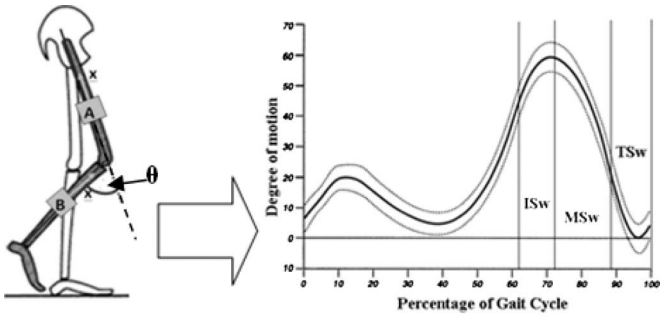

Fig. 3. (a) IMU sensor A and sensor B placed at the thigh and the shank, respectively. (b) Knee angle θ obtained for normal-walking gait.

C. DAQ and Processing

The Inertia Link firmware was designed such that the velocity, acceleration, and Euler angles are transmitted to the USB base station as wireless packets, upon a user command. For the implementation of this system, the user command notifies the sensors to transmit only Euler angles at a sampling rate of 100 Hz [1], [12], [13]. The wireless packet contains 19 B comprising of a header, Euler angles about *x*-, *y*-, and *z*-axes, and a checksum. The software application developed in LabVIEW was programmed to validate the packets received at the host PC, by comparing the transmitted checksum with the received checksum [19].

The FSR signals transmitted voltage values with respect to the force applied on the sensor surface. The literature provided by the manufacturer reported that the part-to-part force repeatability of the FSRs vary from 15% to 25% that could significantly reduce the precision of the measurements. Therefore, to avoid significant inaccuracies of the system, the voltage measurements of individual FSRs placed at the heel, Meta5 and Meta1, and the hallux were obtained for three subjects. The voltage measurements of individual FSR sensors were obtained when the subjects' complete body weight was applied and no weight was applied. These results were used to determine the cutoff values for gait-phase detection, and are further elaborated in the next section.

The FSR sensor signal outputs were sampled at 100 Hz to synchronize the sensor data with the IMUs.

The IMU sensor signals were filtered to remove random noise of the sensor outputs. The moving-average filtering technique was used to obtain a smooth curve of the knee angle to calculate the accurate gradient using the previous five data points. This filtering technique was specifically used due to its simplicity which reduces calculation time, which is essential in real-time applications.

D. FIS for Gait-Phase Detection

Fuzzy controller is a rule-based system in which the condition and the operation are based on fuzzy logic. The conditions and operations are represented as fuzzy sets that define the degree to which a condition is satisfied (membership value (MV)), without drawing a sharp boundary between members and nonmembers of a class. In recent years, researchers have proposed systems based on fuzzy logic and reported key advantages in comparison to other methods as follows.

1) Ng and Chizek [14] reported that gait-event classification based on artificial neural network was significantly poor in comparison to fuzzy-logic-based gait-event detection.
2) Fuzzy logic helps to obtain full information on gait patterns even at the presence of lower sensor signals [16].
3) Fuzzy logic allows smooth transitions even in the presence of rapid changes [16].
4) It has shown to accommodate relatively large step-to-step variability observed in electrically stimulated gait [13].

Furthermore, fuzzy logic is a knowledge-based algorithm that provides a platform to develop a system with an element of explanatory capability on expert rules, and present the data in a manner similar to human thought.

Due to the aforementioned advantages, this paper presents the application of fuzzy logic to determine gait phases with increased simplicity.

The designed FIS consists of only five inputs; the four FSR signals and the knee angle, predefined set of rules and the output, and gait phases. The FIS was implemented such that each gait phase will have an MV of "1" to indicate that the gait phase was completely detected, and an MV of "0" to indicate the gait phase is not detected. If a gait phase has an MV between 0 and 1, it indicates that the gait phase was only partially detected to a degree of the MV.

The gait parameters for each gait phase discussed in Section II-B were used to divide the FSR signals and the knee angle into two categories, namely "high" and "low." "High" and "low" are defined as a function, known as a membership functions (MFs) in fuzzy logic. The MF "high" was defined as a sigmoid function that was used due to its characteristic of being smooth and continuous within a specific range (see Fig. 4). The FSR signals were obtained when the complete body weight was applied and no weight was applied, for several subjects, and the values were averaged to obtain two cutoff values to define the MFs. For example, if the average FSR signal obtained when weight was completely applied and no weight was applied was 4 and 0.8 V, respectively, the sigmoid function was implemented in MATLAB, as represented in Fig. 4. Note, although the FSR signal should be 0 V when no pressure is applied, due to continuous contact of the FSRs and foot, a slight pressure was attained. Similarly, all the FSR inputs were defined as a sigmoid function in MATLAB.

The knee-joint angle was also defined using sigmoid function and the cutoff values were used as 30–40° to illustrate the transition from "low" angle to "high" angle.

The sigmoid function "high" and "low" can be represented as in (1) and (2), in which the values of "*a*" and "*c*" were obtained from the plot of MATLAB, similar to Fig. 4, for each input parameter. f_{High} refers to the MV of an FSR signal that belongs to the "high" MF and *vice versa*

$$f_{\mathrm{High}}(x) = \frac{1}{1 + e^{-1(x-a)}} \tag{1}$$

$$f_{\mathrm{Low}}(x) = 1 - f_{\mathrm{High}}(x). \tag{2}$$

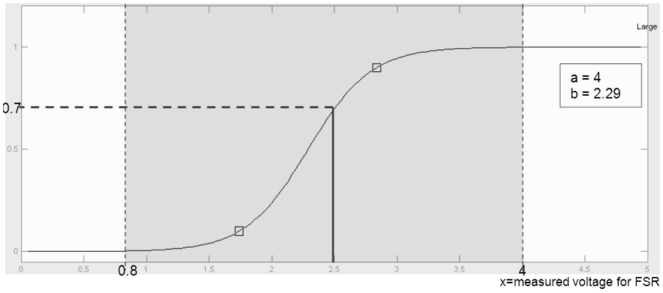

Fig. 4. Example of the fuzzy MF "high" for FSR signals.

TABLE I
PREDEFINED SET OF FUZZY RULES

	FSR 1	FSR 2	FSR 3	FSR 4	Knee angle	Gait Phase
1	High	Low	Low	Low	-	LR
2	High	High	High	Low	-	MSt
3	Low	High	High	High	-	TSt
4	Low	Low	Low	High	-	PSw
5	Low	Low	Low	Low	High	ISw
6	Low	Low	Low	Low	High	MSw
7	Low	Low	Low	Low	Low	TSw

The input MFs were mapped to the output with a minimum number of predefined rules represented in Table I, which were defined based on the foot-pressure patterns and knee-joint angles for each gait phase illustrated in Figs. 2 and 3.

Rule 1 can be further elaborated as "if FSR1 is High AND FSR2 is Low AND FSR3 is Low AND FSR4 is Low, THEN LR." For rule 1 to be satisfied and LR to be detected, all conditions should be satisfied. Here "AND" refers to the maximum MV for each condition. Therefore, for LR to have an MV of "1," FSR1, should completely belong to MF "high" and the rest of the FSR signals should completely belong to MF "low." In other words, referring to (1) and (2) $f_{\mathrm{High}}(FSR1)$, $f_{\mathrm{Low}}(FSR2)$, $f_{\mathrm{Low}}(FSR2)$, and $f_{\mathrm{Low}}(FSR2)$ should have an MV of "1."

These rules were also implemented such that for normal gait, all gait phases will be detected in the sequence starting from LR and ending at TSw.

However, referring to rule 5 and rule 6, it is clear that for the condition where all *FSRs are low* and the *Knee angle is high*, two gait phases, namely ISw and MSw will be detected. This is due to the similar knee-angle values during these two phases. However, it is clear from Fig. 3(b) that the knee angle tends to increase (positive gradient) during ISw, while the knee angle decreases (negative gradient) during MSw. Taking this factor into consideration a new crisp value was introduced into the FIS to distinguish between ISw and MSw. The final FIS consists of five fuzzy inputs and one crisp input.

At certain rules (i.e., rule 4), not all sensor signals were considered to define a gait phase due to the variability of gait parameters for each individual. The clarity of the rules and MF values for the FIS was further tested with data obtained from three subjects performing normal gait. The FIS was refined with these values to optimize and finalize the gait-phase detection algorithm.

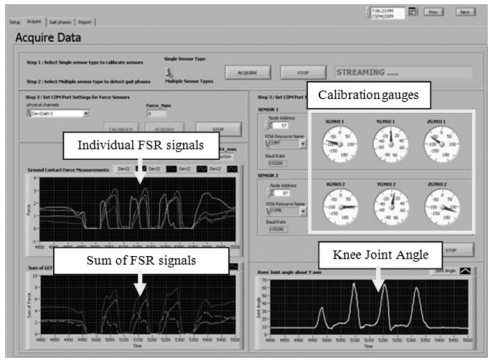

Fig. 5. GUI: DAQ and calibration.

E. Analysis of Gait Phases to Identify Abnormal Gait

The FIS system was implemented such that for normal gait, one gait cycle consists of all gait phases that are detected in the sequence starting from LR and ending at TSw. Furthermore, the FIS was governed by the following criteria for normal gait.

1) Only one gait phase will be detected completely at any given time. This means that only one gait phase will have an MV of "1" at a given instance.
2) For normal gait, the MV of gait phase will be between 0 and 1 only during a transition period from one phase to another.

If the gait phases detected does not comply with the expected sequence and the above criteria, it is safe to report the walking gait as abnormal.

F. Interactive GUI

A main concern in gait analysis is the complexity of dealing with hardware and software and accurate interpretation of gait parameters obtained. Therefore, based on the survey carried out by Lee *et al.* [20] to obtain information on the requirements of gait analysis from a clinician's point of view, GUI was designed to facilitate simplicity to the gait-analysis system. The GUI contains four tabs that allows user to view or add subject information, sensor setup and acquire sensor data, view gait phases detected in a graphical format, and generate a final report based on the gait parameters and gait phases detected.

An important feature in the GUI is the sensor-setup process. This allows the clinicians to perform zero referencing of the IMUs and to test the workability of the sensors before acquisition. The IMU values were displayed on gauges that were identified as a practical representation for zero referencing (see Fig. 5). Upon activating the calibrate button the Euler angles about *Y*-axis will be automatically set to zero.

The GUI is also linked to the database which maintains records of the patients. The user interface facilitates the access to the database without requiring in-depth knowledge on server-side implementation. The overall GUI facilitates the gait-analysis process with minimal functions.

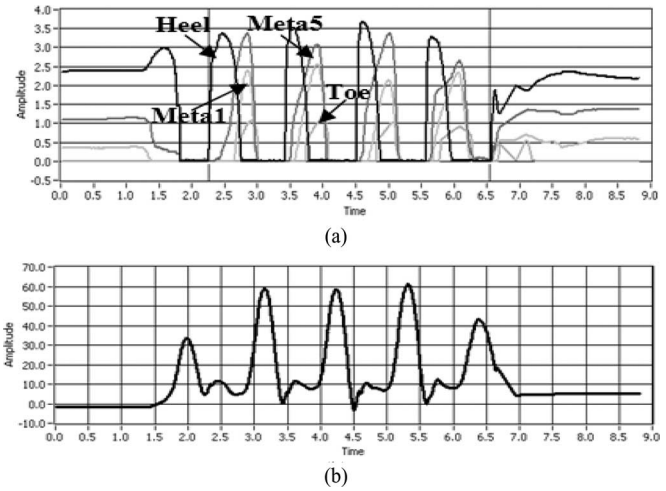

Fig. 6. (a) Foot-pressure patterns and (b) knee-joint angles obtained for normal gait.

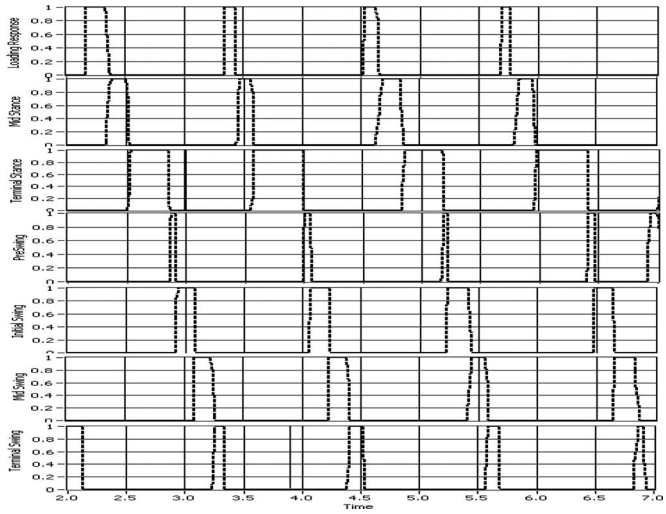

Fig. 7. Gait-phase plots for normal gait.

III. Experimental Setup and Results

A. Experimental Setup

To verify the system developed, three female and three male healthy subjects between ages 22 and 25 years were volunteered. The subjects were asked to wear the shoe insole and the IMUs, as described in Section II-B, to obtain the foot-pressure patterns and the knee-joint angle.

After confirming the comfort of the subjects, they were asked to perform normal-walking gait, and two abnormal gaits at level ground with comfortable speed. The normal-walking trial was recorded for approximately 60 s, and the sensor data were collected to validate the overall system.

The abnormal gait was namely; toe drag and toe walking which are the most common types of knee dysfunctions. Toe drag occurs due to inadequate muscle stimulation to facilitate knee flexion. Low knee flexion during swing phase results the toe to drag on the ground. Toe walking is commonly caused by muscle spasticity that results patients to walk on their toe [6]. During the IC, the forefoot contact occurs without the heel contact.

B. Analysis of Results

The acquired sensor data for a normal-walking gait with five steps are illustrated in Fig. 6 as a function of time in seconds.

The FSR signals and the knee angle closely comply with the expected patterns. However, the first and last gait cycles may be ignored due to occurrence of acceleration and deceleration at the start and end of the gait performance. The gait phases detected for normal gait (see Fig. 7) were in the sequence of LR, MSt, TSt, PSw, ISw, MSw, and TSw that reported a maximum MV of "1" during each gait cycle.

In contrast, all subjects performing toe drag exhibited some of the FSR signals to be detected throughout the gait cycle and the maximum knee flexion reached was significantly less compared to normal gait (see Fig. 8).

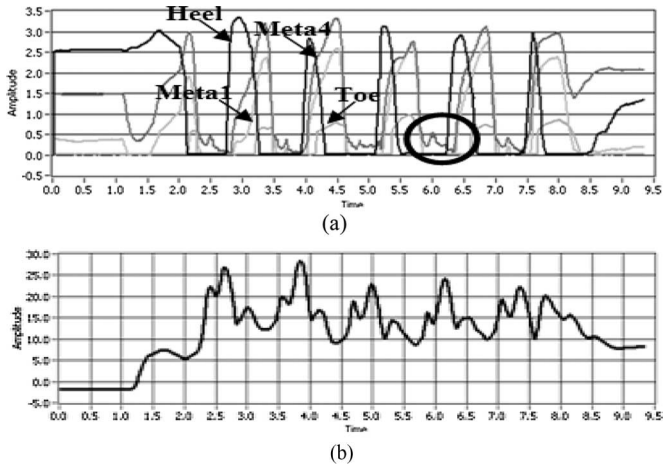

Fig. 8. (a) Foot-pressure patterns and (b) knee-joint angles obtained for toe drag.

Due to some FSR signals being present during swing phase, the rules with condition "*if FSRx is low*" were not fully satisfied. For PSw phase to be detected the FSR at the metatarsal head s are required to be low. For toe drag, these two signals were always "high"; hence, the graphical representation (see Fig. 9) shows the partial detection (MV less than "1") of the phase.

The ISw and the MSw have the condition "*if Knee_angle is high*" in which the "*high*" fuzzy set lie within 40–65°. This condition was not satisfied for toe-drag gait, as the maximum knee angle detected was less than 30° for all subjects. Therefore, the ISw and MSw were not detected for toe-drag gait. Furthermore, TSw was detected twice violating the sequence of the gait phases. This resulted due to the low knee flexion during most of the gait cycle, in turn, satisfying the condition "*Knee_angle is low*," in turn, detecting TSw more than once during each gait cycle.

Toe walking causes a walking gait cycle to not have heel contact during the stance phase. As a result, the FSR placed at the heel will always have a value close to zero (see Fig. 10(a)).

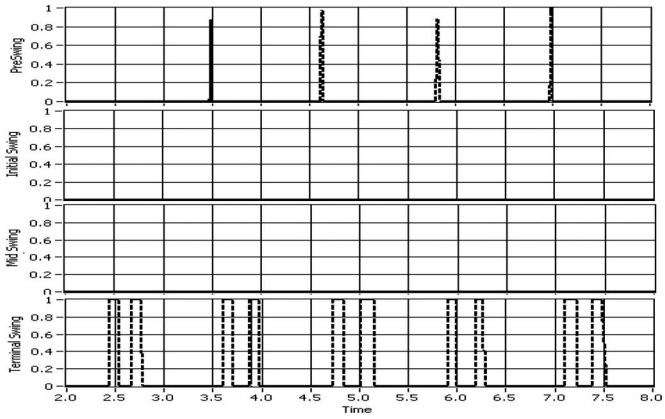

Fig. 9. Gait-phase plots for toe drag.

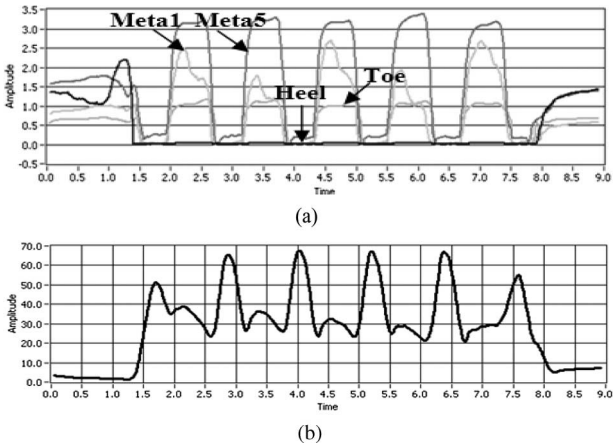

Fig. 10. (a) Foot-pressure patterns and (b) knee-joint angles obtained for toe walking.

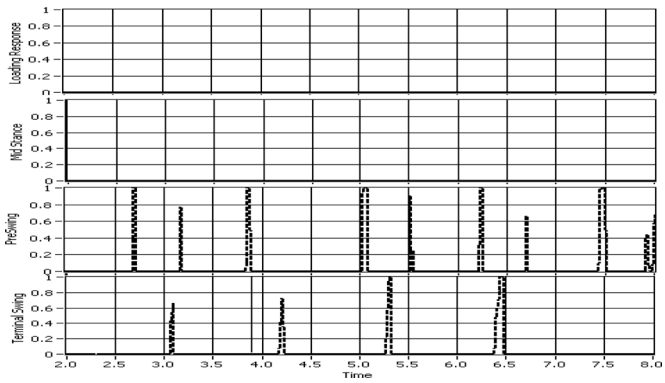

Fig. 11. Gait-phase plots for toe walking.

No heel contact also restricts the knee from reaching maximum extension. Most subjects performing toe walking illustrated a maximum extension within 9–25° (see Fig. 10(b)). Therefore, rules with the condition "*FSR1 is high*" and "*Knee is small*" were not completely satisfied, causing LR, MSt, and TSw to only be detected partially or not detected at all (see Fig. 11). The PSw phase was also detected in an irregular manner throughout toe-walking gait because the "*FSR4 is high*" condition was true throughout stance phase.

In contrast to existing systems, the proposed algorithm could also aid in identifying the instances of the deformity occurrence. For instance, for toe-drag gait, it is safe to conclude that the deformity did not occur during the MSt and TSt phases because they were completely detected in the expected sequence. Therefore, the problem occurrence can be narrowed down to the remaining gait phases that were partially or completely undetected.

In contrast to a threshold method, the output of the gait phases detected are smooth and does not rapidly change from "1" to "0" or *vice versa*. This could provide a safe platform for using the proposed system to control feedback devices.

The FIS detected all gait phases in the expected sequence during normal gait. Therefore, the detection reliability of the system for a total of 270 steps (45 steps $\times$ 6 subjects) was 100%. In [6], the gait phases LR, MSt, TSt, PSw, ISw, MSw, and TSw are represented as 10%, 20%, 20%, 10%, 13%, 14%, and 13% of the gait cycle, respectively. These percentages were used to calculate the expected time durations (reference time durations) each gait phase should be detected for each gait cycle. Based on these data, the error difference between the normative data and the gait phases detected during each system was calculated. The calculation of error for LR phase is represented as follows:

$$\text{Error (in milliseconds)} = \left[\left(\frac{\mathrm{GC_{time}} \times \%\mathrm{LR})}{100}\right) - \mathrm{LR\_of\_FIS_{time}}\right] \quad (3)$$

where GC, where $\mathrm{GC_{time}} = \mathrm{gaitcycletime}$, and %LR is the accepted percentage of LR phase within one gait cycle.

Hence, the average error and standard deviations reported for LR, MSt, TSt, PSw, ISw, MSw, and TSw are 11 ± 92, 57 ± 113, -67 ± 58, 66 ± 44, 5 ± 26, -12 ± 25, and 64 ± 29 ms, respectively. The error was reported as positive when the FIS detected a gait phase for a less time period that the standard accepted time and *vice versa*.

The duration of the gait phases obtained from the FIS was calculated as a percent of the gait cycle to further quantify the accuracy of the FIS. The difference between the percentage of gait phase obtained from the FIS and the normative data were calculated to obtain the error as a percentage difference. The average error as a percentage difference obtained for 45 steps for all subjects are tabulated in Table II.

IV. Discussion and Conclusion

As an overall analysis of the system, most of the errors as well as the variations occurred during the stance phase, indicating inaccuracies due to foot-pressure measurements. The errors may have been caused by different shoe sizes of the subjects participated. Although the shoe insole used was of size 8, the subjects volunteered in this study were of shoe sizes 6–11. Therefore, the placements of the sensors may not have been placed accurately under the heel, metatarsal heads, and toe as expected. For example, referring to LR phase, subjects with smaller shoe sizes

TABLE II
DIFFERENCE BETWEEN THE GAIT PHASES OBTAINED FROM THE FIS AND THE NORMATIVE DATA, AS AN AVERAGE FOR 45 STEPS FOR EACH SUBJECT (THE ERRORS ARE REPORTED AS A PERCENTAGE DIFFERENCE)

Subject	LR (%)	MSt (%)	TSt (%)	PSw (%)	ISw (%)	MSw (%)	TSw (%)
A	-9	14	-5	6	-2	-1	6
B	4	-9	0	7	3	-1	3
C	0	3	-7	5	0	-2	6
D	-12	13	-4	7	2	-2	7
E	6	-3	-12	8	-1	0	8
F	6	10	-5	0	1	1	2

(subject A with shoe size 7, and subject D with shoe size 6) resulted in errors with negative percentages, indicating that the phase was detected longer compared to normative data, while subjects with bigger shoe sizes (subjects B, E, and F) resulted in errors with positive percentages, indicating the phase was detected for a shorter duration compared to normative data. This is because the rule specifies that the LR phase is detected only when FSR1 is "high" and the rest are "low". As soon as FSR2 and FSR3 reach the cutoff values, MSt phase reports an MV of greater than "0." For subjects with smaller shoe sizes, the time taken for FSR2 and FSR3 to reach the cutoff values is more, hence resulting in longer periods of LR phase in comparison to those with larger shoe sizes. The rest of the inaccuracy occurrence can also be explained in the similar manner. The subject C, with shoe size $8\frac{1}{2}$, which is the closest to the instrumented shoe insole reported gait-phase percentages closest to the normative data. The minimum error differences varying between -7% and 6% during the stance phase was reported for this subject (root-mean square $= 62$ ms for 45 steps). This further clarifies that most errors were due to different shoe sizes of the test subjects. Therefore, errors could be significantly reduced by developing shoe insoles to match the exact size of the participant.

A comparative study was carried out based on key research addressed in the literature for gait-phase detection. The maximum error reported for the proposed system was less in comparison to the algorithms proposed by Skelly and Chizek [13] and Pappas *et al.* [1]. Smith *et al.* [11] reported a maximum error of 12 ms less than the proposed system. However, an average variability of more than 80 ms was reported for all gait phases that was much higher than the proposed system.

More sophisticated techniques such as supervised machine-learning techniques [12] and hybrid intelligent systems [15] could further improve the accuracy of the gait-phase detection algorithm. However, the complexity of such systems may cause the overall system to increase computational time, which is a major drawback in real-time applications.

The results show that the developed system was able to identify abnormalities based on the gait phases detected and aid in identifying the point of abnormality occurrence. Hence, people with normal gait could benefit from the system, to detect the presence of slowly occurring abnormalities, while people with pathological gait could benefit from the system in terms of identifying accurate timing for corrective feedback.

REFERENCES

[1] I. P. Pappas, T. Keller, S. Mangold, M. R. Popovic, V. Dietz, and M. Morari, "A reliable gyroscope-based gait phase detection sensor embedded in a shoe insole," *IEEE Sensors J.*, vol. 4, no. 2, pp. 268–274, Apr. 2004.

[2] R. Luo and Y. C. Yeh, "Sensory controlled intelligent assistant system for walking rehabilitation," in *Proc. IEEE 2002 28th Annu. Conf. IECON*, Nov., vol. 2, pp. 1573–1578.

[3] S. Bamberg, A. Y. Bensabat, D. M. Scarborough, D. E. Krebs, and J. A. Paradiso, "Gait analysis using a shoe integrated wireless sensor system," *IEEE Trans. Inf. Technol. Biomed.*, vol. 12, no. 4, pp. 413–423, Jul. 2008.

[4] J. W. Fee, F. Miller, N. Lennon, A. Hosp, and D. Wilmington, "EMG reaction in muscles about the knee to passive velocity, acceleration and jerk manipulations," *J. Electromyogr. Kinesiol.*, vol. 19, pp. 467–475, Jun. 2009.

[5] A. Stefano, J. Burrudge, V. Yule, and R. Allen, "Effect of gait cycle selection on EMG analysis during walking in adults and children with gait pathology," *Gait Posture*, vol. 20, pp. 92–101, Aug. 2004.

[6] J. Perry, *Gait Analysis: Normal Gait and Pathological Function*. Thorofare, NJ: Slack, 1999, ch. 1–6.

[7] M. Nordin and V. H. Frankel, *Basic Biomechanics of the Musculoskeletal System*, 3rd ed. Baltimore, MD: Lippincott Williams and Wilkins, 2001, ch. 7–9.

[8] R. Bartlett, *Introduction to Sports Biomechanics: Analysing Human Movement Patterns*, 2nd ed. London, U.K./NY: Taylor and Francis, 2007, ch. 1.

[9] R. Heliot, R. Pissard-GiboIIet, B. Espiau, and F. Favre-Reguilion, "Continuous identification of gait phase for robotics and rehabilitation using microsensors," in *Proc. 12th Int. Conf. Adv. Robot.*, 2005, pp. 686–691.

[10] J. H. Choi, J. Cho, J. H. Park, J. M. Eun, and M. S. Kim, "Efficient gait phase detection devices based on magnetic sensor array," in *Proc. IFMBE, 4th Kuala Lampur Int. Conf. Biomed. Eng.*, 2008, vol. 21, pp. 778–781.

[11] B. T. Smith, D. J. Coiro, R. Finson, R. R. Betz, and J. McCarthy, "Evaluation of force-singing resistoes for gait event detection to trigger electrical stimulation to improve walking in the child with cerebral palsy," *IEEE Trans. Neural Syst. Rehabil. Eng.*, vol. 10, no. 1, pp. 22–29, Mar. 2002.

[12] R. Williamson and B. J. Andrews, "Sensor systems for lower limb functional electrical stimulation (FES) control," *Med. Eng. Phys.*, vol. 22, pp. 313–325, 2000.

[13] M. M. Skelly and H. J. Chizek, "Real time gait event detection for parapligic FES walking," *IEEE Trans. Neural Syst. Rehabil. Eng.*, vol. 9, no. 1, pp. 59–68, Mar. 2001.

[14] S. K. Ng and H. J. Chizek, "Fuzzy model identification for classification of gait events in paraplegics," *IEEE. Trans. Fuzzy Syst.*, vol. 5, no. 4, pp. 536–544, Nov. 1997.

[15] R. Lauer, B. T. Smith, and R. R. Betz, "Application of a neuro-fuzzy network for gait event detection using electromyography in the child with cerebral palsy," *IEEE Trans. Biomed. Eng.*, vol. 52, no. 9, pp. 1532–1540, Sep. 2005.

[16] K. Kong and M. Tomizuka, "Smooth and continuous human gait phase detection based on foot pressure patterns," presented at the IEEE Int. Conf. Robot. Autom., Pasadena, CA, May 19–23, 2008.

[17] K. Kong, J. Bae, and M. Tomizuka, "Detection of abnormalities in a human gait using smart shoes," presented at the SPIE Smart Struct./NDE, Health Monit., San Diego, CA, 2008.

[18] *FSR Integration Guide*, Interlink Electron., Camarillo, CA, 2000.

[19] *3DM-GX2 Data Communication Protocol*, Microstrain Inc., Williston, VT, 2007.

[20] M. Lee, M. Rittenhouse, and H. A. Abdullah, "Design issues for therapeutic robot systems: Results from a survey of physiotherapists," *J. Intell. Robot. Syst.*, vol. 42, pp. 239–252, 2005.

Authors' biographies and photographs not available at the time of publication.